RESPONSE OF A CYLINDRICAL SHELL TO RANDOM ACOUSTIC EXCITATION

by
Daniel D. Kana

INTERIM REPORT
Contract No. NAS8-21479
Control No. DCN 1-9-53-20039 (1F)
SwRI Project No. 02-2396

Prepared for

National Aeronautics and Space Administration
George C. Marshall Space Flight Center
Huntsville, Alabama

15 July 1969

SOUTHWEST RESEARCH INSTITUTE
SAN ANTONIO HOUSTON

SOUTHWEST RESEARCH INSTITUTE
Post Office Drawer 28510, 8500 Culebra Road
San Antonio, Texas 78228

RESPONSE OF A CYLINDRICAL SHELL TO RANDOM ACOUSTIC EXCITATION

by
Daniel D. Kana

INTERIM REPORT
Contract No. NAS8-21479
Control No. DCN 1-9-53-20039 (1F)
SwRI Project No. 02-2396

Prepared for

National Aeronautics and Space Administration
George C. Marshall Space Flight Center
Huntsville, Alabama

Approved:

H. Norman Abramson, Director
Department of Mechanical Sciences

ABSTRACT

Response and equivalent force spectra have been investigated for random acoustic excitation of a cylindrical shell within a frequency band of relatively low modal density. Theoretical and experimental results are compared for single point transfer functions, acoustic mobility functions, response and equivalent force power spectral densities, and coherence functions. In general, it is found that a purely theoretical prediction of response based on linear random process theory is severely limited because of the inability of currently available expressions for transfer functions to account for various deviations which result principally from imperfections and eccentricities in the cylinder. However, good agreement is achieved between measured response and that calculated with measured transfer functions. It is further indicated that a rather coarse discrete representation of a continuously distributed excitation is possible.

TABLE OF CONTENTS

	Page
GENERAL NOTATION	iv
LIST OF ILLUSTRATIONS	v
INTRODUCTION	1
ANALYTICAL EXPRESSIONS	3
Response to Multiple Discrete Excitation	3
Equivalent Force Spectra	5
EXPERIMENTAL PROCEDURES AND RESULTS	8
Measurement of Excitation Field	8
Harmonic Excitation and Response	13
Random Excitation and Response	19
ACKNOWLEDGMENTS	33
REFERENCES	34
APPENDIX	35

GENERAL NOTATION

a	shell radius
B_e	equivalent filter bandwidth for spectral density analysis
f	analysis frequency, Hz
h	thickness of shell wall
ℓ	shell length
n_e	statistical degrees of freedom for spectral density analysis
RC	averaging time constant for spectral density analysis
ρ_s	shell mass density
ω	excitation circular frequency
ω_{mn}	natural frequency of m, n-th mode

LIST OF ILLUSTRATIONS

1. Coordinate System
2. Apparatus for Measuring Acoustic Field
3. Cross-Spectral Densities of Acoustic Field
4. Spatial Distribution of Acoustic Field
5. Apparatus for Point Excitation of Cylinder
6. Transfer Function Between Y1 and x = (0, 0)
7. Transfer Function Between Y1 and x = (4, 0)
8. Acoustic Mobility Function for Y1
9. Transfer Function Between Y2 and x = (0, 0)
10. Transfer Function Between Y2 and x = (4, 0)
11. Acoustic Mobility Function for Y2
12. Single Point Random Response for Y1
13. Acoustic Random Response for Y1
14. Acoustic Random Response for Y2
15. Theoretical Equivalent Force Spectra for Y1 and Y2
16. Variation of Acoustic Response at Y1 with Excitation Mesh Size
17. Coherence Function for Random Excitation

INTRODUCTION

Dynamic loading on launch and space vehicle structures is comprised to a great extent of spatially-distributed random acoustic energy which is generated by various sources within the vehicle environment. At launch, high-level engine noise is reflected from the ground up onto the structure, while during flight aerodynamic turbulence as well as engine noise excite structural response. This response is important from the point of view of its influence on internal components and systems in addition to that of structural integrity itself. Since cylindrical shells are a typical component in current structural designs, it is particularly important that their response to such distributed loads be understood.

A general analytical approach to determine the response of elastic structures to distributed random excitation has been given by Robson[1] as well as others. The essence of this approach involves first the determination of theoretical structural admittances or transfer functions between response at some appropriate point and harmonic excitation at a single point. These functions can conveniently be expressed as series expansions of the normal modes of the system. Then, by means of generalized harmonic analysis and superposition properties of linear random process theory, expressions are obtained which relate statistical properties of the response to the transfer functions and statistical properties of the excitation over the aggregate of points in the area over which a distributed load acts. This approach has been applied to the case of certain types of random

response of a cylindrical shell by Nemat-Nasser[2], and more recently by Hwang[3]. It is very evident from these analyses that the particular form of damping mechanism which is assumed has a profound influence on the response, as it does in any force vibration problem. It is further apparent that no modal distortions, and thereby deviations in response distributions, such as may be caused by eccentricities in the cylinder, can be predicted by such a theory.

In view of the fact that previous investigations[4] of dynamic shell behavior under harmonic excitation have uncovered various deviations of response from that predicted by normal modal theories, an experimental program was conducted to determine the validity of such theories as applied to the case of random excitation as well as to investigate several concepts important to the design of environmental tests for internal systems which may be attached to the shell. The results of this work are presented herein. For convenience, first a discussion of appropriate analytical relationships between excitation and response are given for the cylindrical shell. These are presented in a form for synthesizing a continuously distributed load into a gridwork of multiple discrete loads, so that information on the required mesh density for such a procedure can be obtained. Then, expressions are given for replacing the distributed load by an equivalent concentrated random load acting at the response point. Both of these concepts are of eminent importance in the design of force spectra for environmental testing of internal systems.

ANALYTICAL EXPRESSIONS

Response to Multiple Discrete Excitation

It will be of convenience to decompose a continuously distributed random acoustical load into an aggregate of multiple discrete loads. For such a representation in a linearly elastic structure, the following matrix relationship can be written[5] between excitation and response:

$$S_{yy}(f) = (H_{xy})\,[S_{xx}]\,\{H_{xy}^{*}\} \qquad (1)$$

where

$S_{yy}(f)$ = displacement power spectral density of the response at y

(H_{xy}) = row vector of displacement admittance at y to force applied at x

$[S_{xx}]$ = square matrix of cross-spectral densities of excitation forces at various discrete points

$\{H_{xy}^{*}\}$ = column vector of complex conjugates of elements of (H_{xy}).

The use of any transfer function in Eq. (1) is valid; here, however, displacement is chosen merely for convenience. For a purely theoretical application of this equation analytical expressions must be utilized for the admittance functions. Analogous to Sec. (4.7) of Robson[1] for a cylindrical shell with coordinate system as indicated in Figure 1, the following displacement admittance between a lateral excitation at x and displacement at y can be obtained:

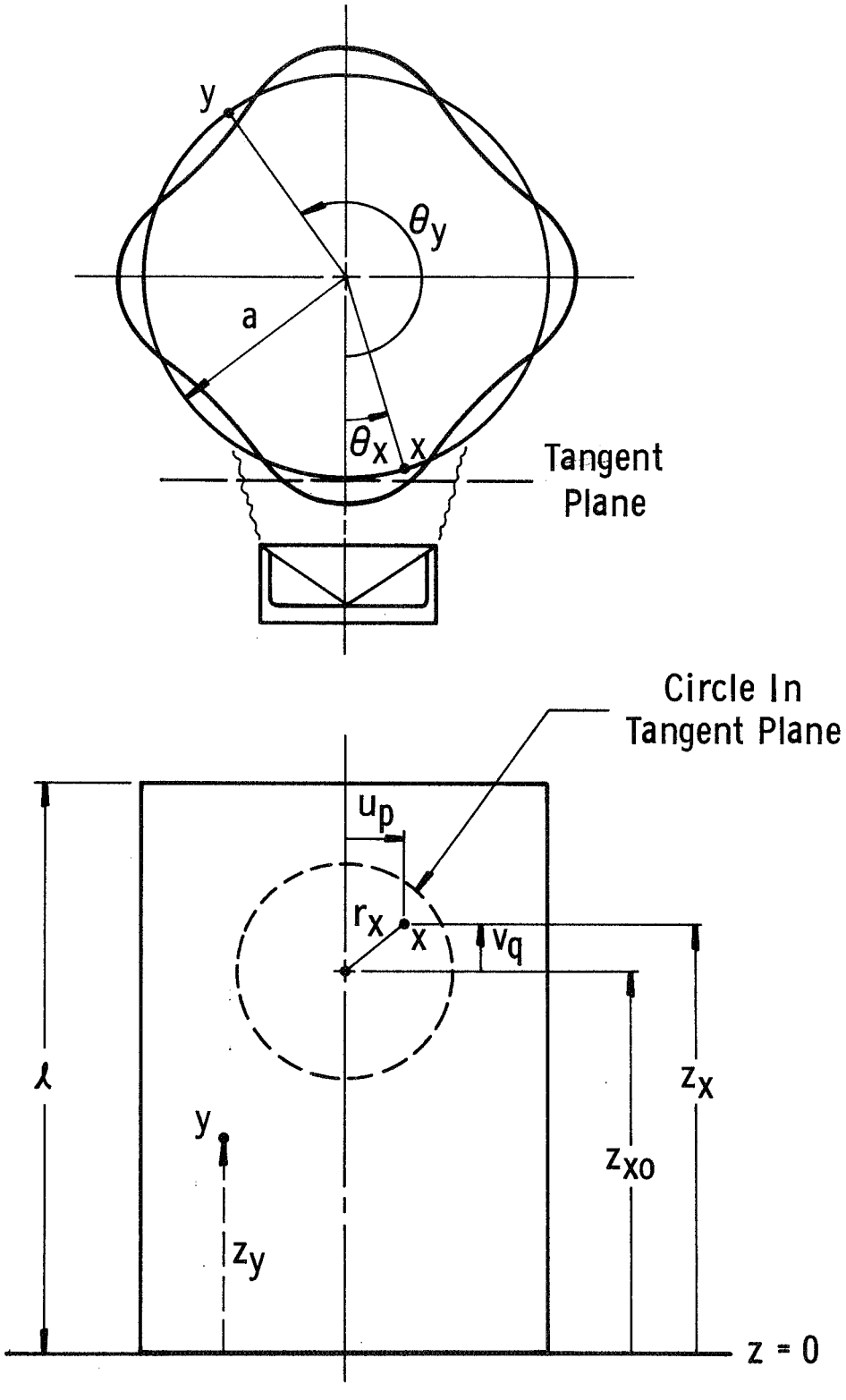

Figure 1. Coordinate System

$$H_{xy} = \sum_{1}^{m}\sum_{n} \frac{w_{mn}(z_y, \theta_y-\theta_x)\, w_{mn}(z_x, \theta_x=0)\,(1-\zeta^2-i\eta_{mn})}{M_{mn}\omega_{mn}^2\,[(1-\zeta^2)^2+\eta_{mn}^2]} \qquad (2)$$

where

$$\zeta = \omega/\omega_{mn}$$

and

$$M_{mn} = \rho_s h a \int_0^{\ell}\int_0^{2\pi} w_{mn}^2\,(z,\theta)\; dz d\theta$$

For a simply-supported cylinder

$$w_{mn}(z,\theta) = \sin\frac{m\pi z}{\ell}\cos n\theta \qquad (3)$$

so that

$$M_{mn} = \rho_s h\left(\frac{a\pi\ell}{2}\right)$$

It should be noted that a structural type of damping has been specified, and that the response pattern is assumed to follow the point x of load application so that

$$w_{mn}(z_x, \theta_x) = \sin\frac{m\pi z_x}{\ell} \qquad (4a)$$

$$w_{mn}(z_y, \theta_y-\theta_x) = \sin\frac{m\pi z_y}{\ell}\cos n(\theta_y-\theta_x) \qquad (4b)$$

The latter behavior occurs in a perfectly symmetrical cylinder.

Equivalent Force Spectra

In order to determine the power spectral density of a single excitation force acting at point y in such a way as to replace the effects of the distributed or multiple discrete load, and to allow for the additional reaction effects of an internal system package, it is first necessary to develop several admittance relationships. Assuming steady-state harmonic

excitation and response, we introduce the following notation:

$F_y(f)$ = amplitude of applied excitation at y

$G_y(f)$ = amplitude of reaction force of internal system at y

$W_y(f)$ = displacement of shell at y when internal system is attached

$W_{yF}(f)$ = displacement of shell at y due to force $F_y(f)$ when internal system is detached

$W_{yG}(f)$ = displacement of shell at y due to the action of $G_y(f)$ alone

$H_{\ell\ell}(f)$ = driving point admittance of internal system

$H_{yy}(f)$ = driving point admittance at point y of shell only with internal system detached

The complex admittance functions may be defined as having zero phase angle when displacement and force act in the same direction. Thus, for the cylinder and attached internal system we can write

$$W_y(f) = W_{yF}(f) + W_{yG}(f) \tag{5}$$

but

$$W_{yF}(f) = H_{yy}(f)\, F_y(f) \tag{6a}$$

$$W_{yG}(f) = -H_{yy}(f)\, G_y(f) \tag{6b}$$

and

$$G_y(f) = W_y(f)/H_{\ell\ell}(f) \tag{6c}$$

Upon substitution of Eqs. (6) into (5) and solving for $G_y(f)$, there results

$$G_y(f) = F_y(f) \left[\frac{H_{yy}(f)}{H_{yy}(f) + H_{\ell\ell}(f)} \right] \tag{7}$$

These expressions are valid for steady state harmonic excitation. For the case of random excitation, by means of generalized spectral analysis[5], Eqs. (6a) and (7) become

$$S_F(f) = \left|H_{yy}\right|^{-2} S_{yy}(f) \tag{8a}$$

$$S_G(f) = \left| \frac{H_{yy}(f)}{H_{yy}(f) + H_{\ell\ell}(f)} \right|^2 S_F(f) \tag{8b}$$

It can be seen from Eqs. (8a) and (1) that $S_F(f)$ is an equivalent concentrated force spectra which acts at y in such a way as to produce the same response $S_{yy}(f)$ of the shell alone as that of a distributed load. Further, $S_G(f)$ is the force spectra to which the internal system alone must be subjected in order to duplicate the environment it must withstand as a result of the action of the distributed load on the shell.

EXPERIMENTAL PROCEDURES AND RESULTS

Measurement of Excitation Field

In order to employ Eq. (1) for prediction of shell response it is necessary to determine the elements of the matrix $[S_{xx}]$ for a given distributed load. That is, the properties of the acoustic excitation field must be measured. For this purpose, a microphone was mounted in a simulated cylindrical section and placed in the same position relative to the acoustical speaker as that to be used when exciting the actual cylinder. Both the cylindrical section and the cylinder had the same radius. A photograph of this part of the apparatus is shown in Figure 2. The microphone and section could be moved vertically and swung horizontally, while the speaker was driven by a Gaussian noise generator.

Thus, the speaker output was measured over its entire effective field, and recorded on analog tape. The subsequent data was then processed by means of analog spectral analysis equipment in order to determine its statistical properties. Samples of the cross-PSD between the acoustic pressure at the speaker centerline and other off-center positions are shown in Figure 3 for a limited frequency band. It is implied from the figure that the imaginary part of the ordinarily complex functions was essentially zero. From such data it was determined that the excitation field was of purely convective form, was essentially symmetrical, and that the elements of $[S_{xx}]$ were

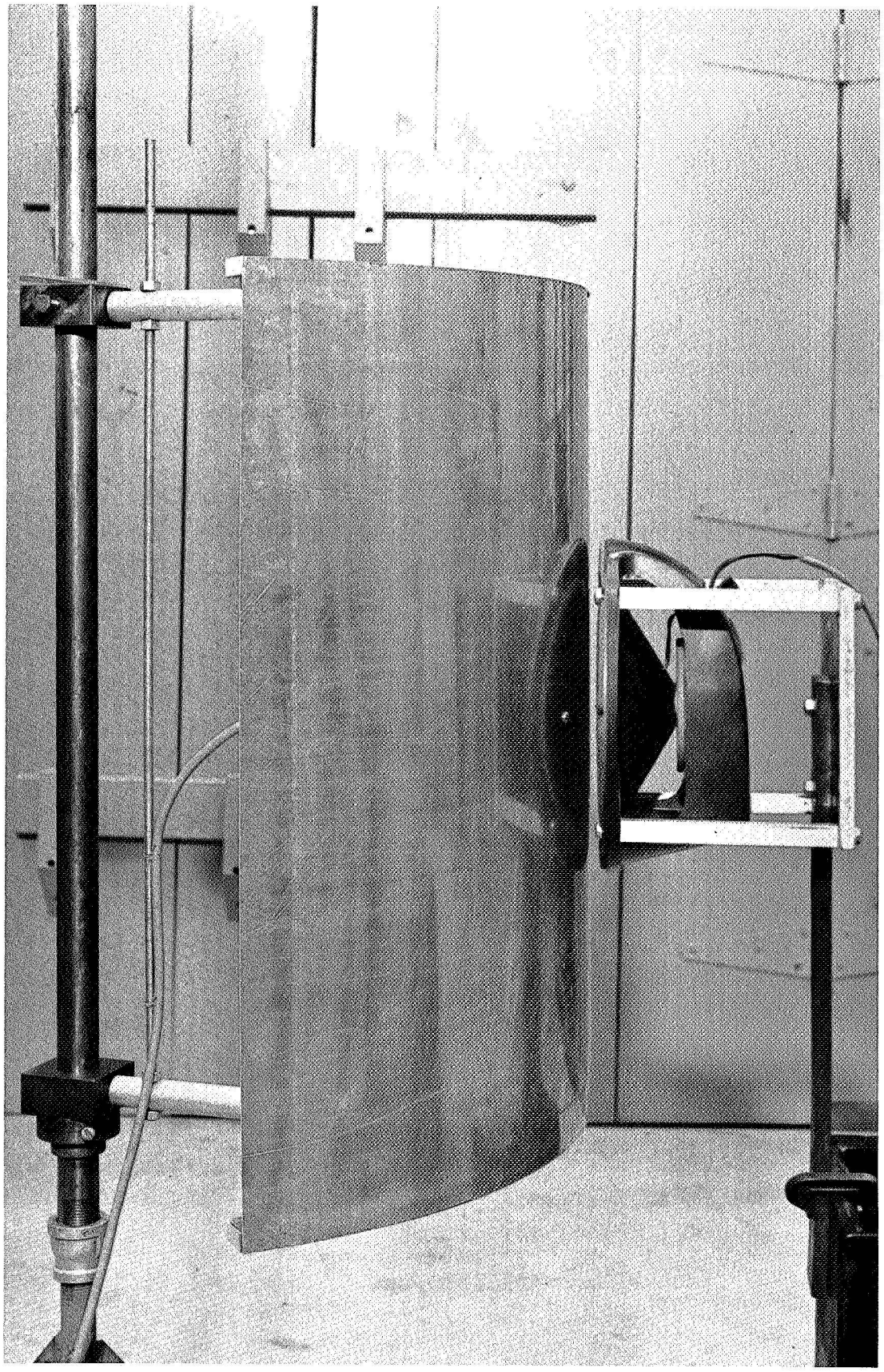

Figure 2. Apparatus For Measuring Acoustic Field

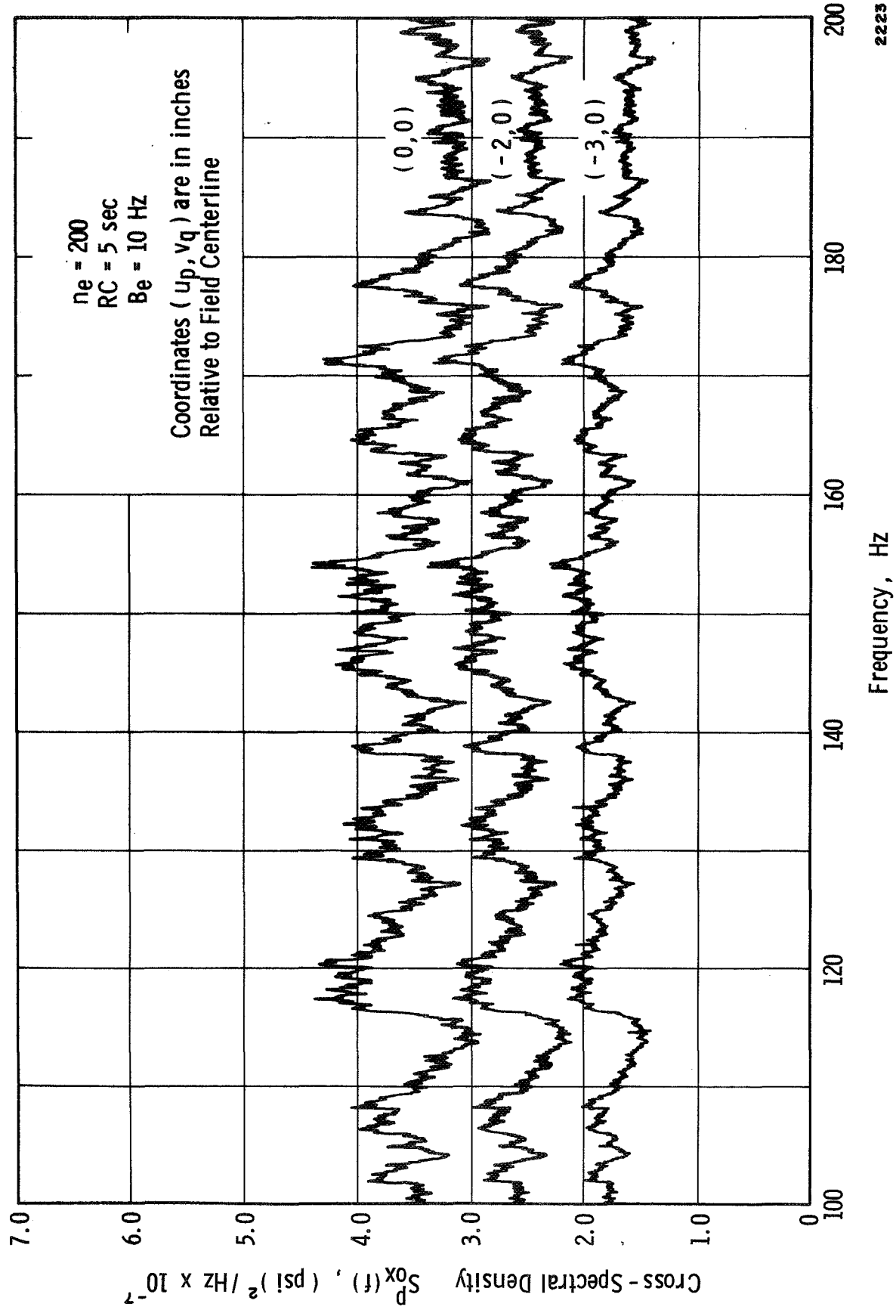

Figure 3. Cross-Spectral Densities Of Acoustic Field

$$S_{xx}(f) = k_x^2 \, S_{00}(f) \tag{9a}$$

$$S_{x_1x_2}(f) = S_{x_2x_1}(f) = k_{x_1} k_{x_2} \, S_{00}(f) \tag{9b}$$

where

$$k_x = e^{-[(r_x^{2.682})/28.8]} \tag{10}$$

and r_x is the radial distance off the speaker axis in a plane tangent to the cylinder as shown in Figure 1. Further, $S_{00}(f)$ is the force PSD of the excitation at the point of intersection of the speaker centerline with the tank wall. Equation (10) is an empirical relationship which has been fit to the experimental data as shown in Figure 4. This type of directly correlated excitation field is discussed on pp. 77-81 of Robson[1]. For this case, Eq. (1) reduces to

$$S_{yy}(f) = \left|\alpha_{xy}^p\right|^2 \, S_{00}^p(f) \tag{11}$$

where

$$\alpha_{xy}^p = \Delta^2 \sum_p^N \sum_q^N k_x \, H_{xy} \tag{12}$$

is defined as an acoustical mobility function, Δ is the gridwork mesh size, and $S_{00}^p(f)$ is the pressure power spectral density measured at the intersection of the centerline of the speaker with the shell.

For later calculations, it was determined from Figure 3 that at $(u_p, v_q) = (0, 0)$ we have

$$S_{00}^p(f) = 3.66 \times 10^{-7} \text{ psi}^2/\text{Hz}$$

as an average value throughout the frequency range of 100 to 180 Hz.

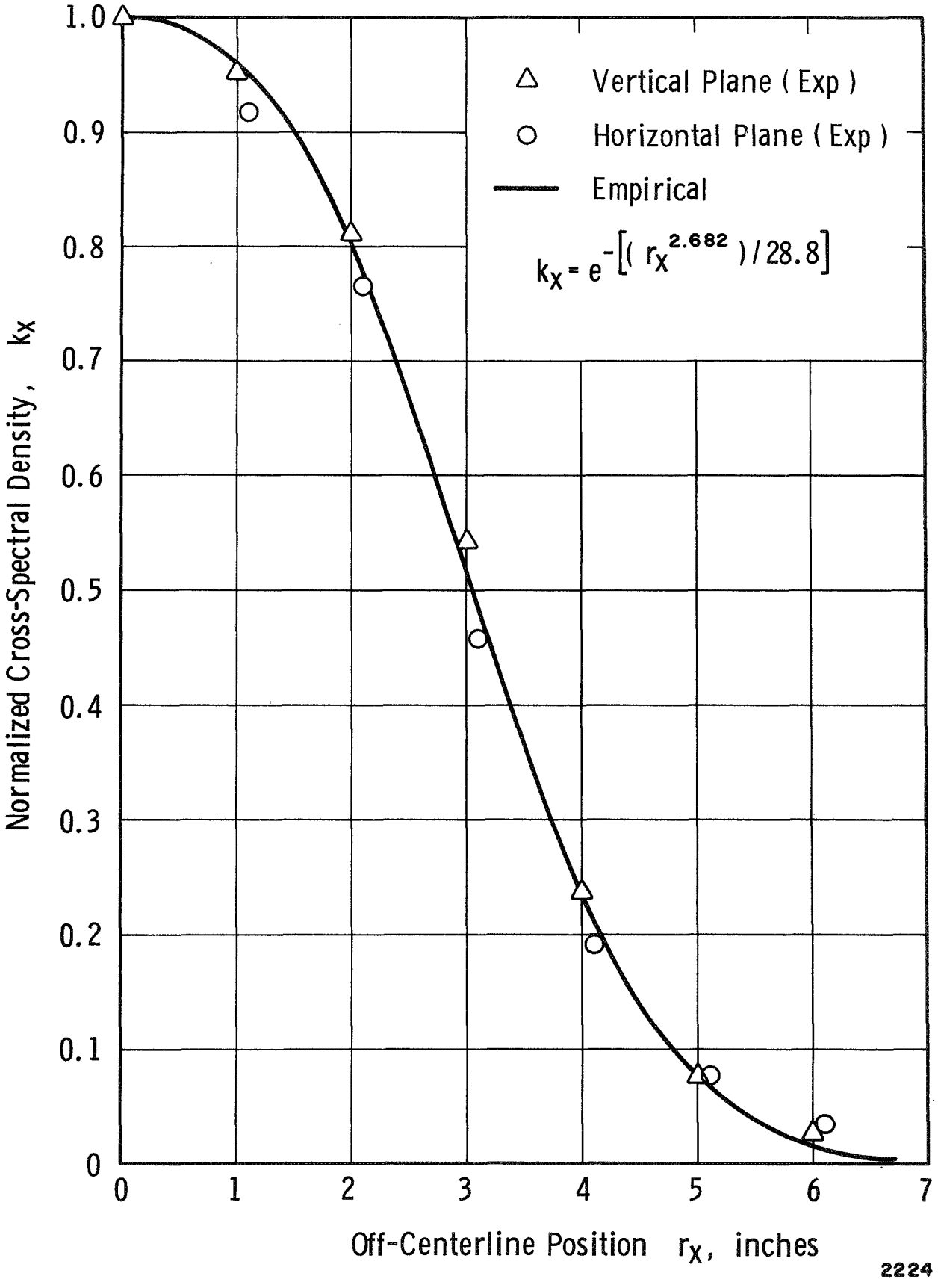

Figure 4. Spatial Distribution Of Acoustic Field

Further, for single point excitation to be described later, the same taped signal was utilized to drive a point electrodynamic coil at a value of

$$S_{00}(f) = 1.26 \times 10^{-5} \text{ lb}^2/\text{Hz}$$

Harmonic Excitation and Response

Experiments with harmonic excitation of a cylinder were conducted both with single-point and distributed acoustic excitation in order to measure transfer (or admittance) functions and to observe the qualitative behavior of the system. The apparatus for single-point excitation is shown in Figure 5. The electrodynamic shaker has a moving element of only 8 gm. which is attached to the cylinder. Thus, mass loading effects were negligible in the frequency range of interest. A noncontacting Bentley transducer was used for measuring displacement (not shown in the photograph). The cylinder is attached to the end skirts primarily for ease in handling, and the combination is bolted to a solid closed base as shown, but is open at the top.

The cylinder shown in Figure 5 is the same as that used in a previous study[4], except that no bulkheads were incorporated for the present experiments. Properties of this cylinder along with some experimentally measured natural frequencies are given in Table I. Damping factors η_{mn} were determined by measuring the transfer function for harmonic single-point excitation at the various natural frequencies and observing the displacement with the following parameters:

$\theta_x = 0°$ $\qquad$ $\theta_y = 180°$

$z_x = 15$ in. $\qquad$ $z_y = 12.5$ in.

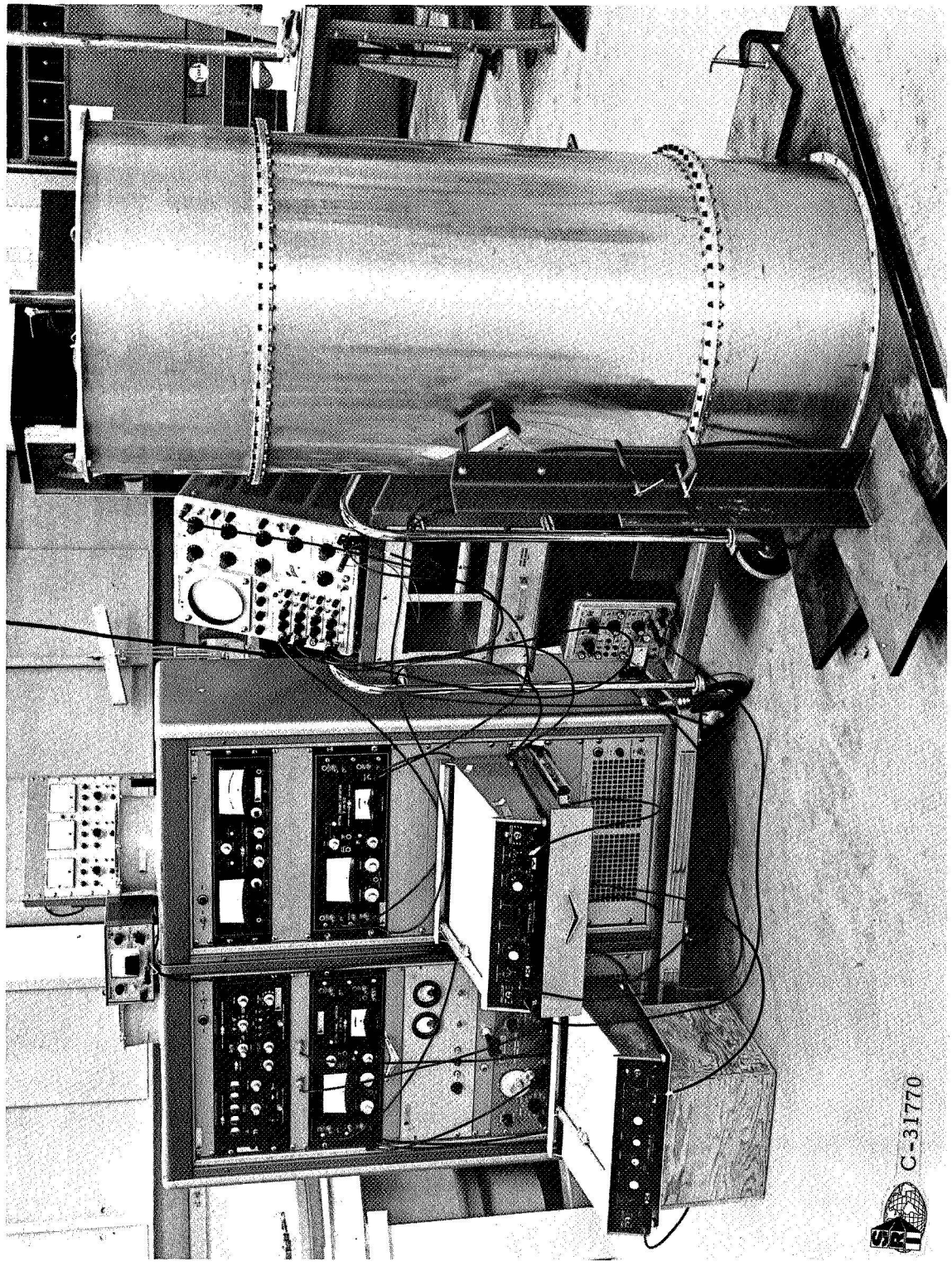

Figure 5. Apparatus For Point Excitation Of Cylinder

TABLE I

PROPERTIES AND
NATURAL FREQUENCIES OF TEST CYLINDER

$\rho_s = 2.59 \times 10^{-4}$ lb sec^2/in^4 a = 12.42 in.

h = 0.020 in ℓ = 15.0 in.

MODE m	MODE n	FREQUENCY Hz	DAMPING FACTOR η_{mn}
1	5	214.7	0.00668
1	6	176.1	0.00922
1	7	144.5	0.01870
1	8	132.8	0.00977
1	9	137.2	0.00386
1	10	150.4	0.01380
1	11	168.0	0.01080
1	12	193.9	0.00531
1	13	224.8	0.00884
2	10	237.0	
2	11	241.0	
2	12	244.0	
2	13	259.0	

The measured force and displacements were then substituted into Eq. (2) so that the various η_{mn} could be calculated. The summations in Eq. (2) were neglected for this purpose. This simplification is valid only for well separated modes and low damping. It is obvious from Table I that the damping factors are dependent on frequency, a result which is not predicted by simple structural damping theory.

Transfer functions were measured over a frequency band which included several of the lower natural frequencies and the results were compared with numerical results computed from Eq. (2) including the damping factors given in Table I. The lowest nine modes were used for the series expression.

A comparison of results for one response point (Y1) and two different excitation points is given in Figures 6 and 7. Co and Quad refer respectively to the real and imaginary parts of the transfer function. It is obvious from the two figures that the modal pattern does indeed shift relative to the space fixed coordinate system as the excitation point is moved around the circumference of the cylinder. However, discrepancies between theoretical and experimental results further indicate that some distortion of modal patterns also occurs. Nonalignment of peaks in the theoretical and experimental Quad part of the transfer functions indicates that slightly different resonant frequencies can be obtained by observing response at different points. Perfect alignment can be achieved only when the point of observation for experimental response

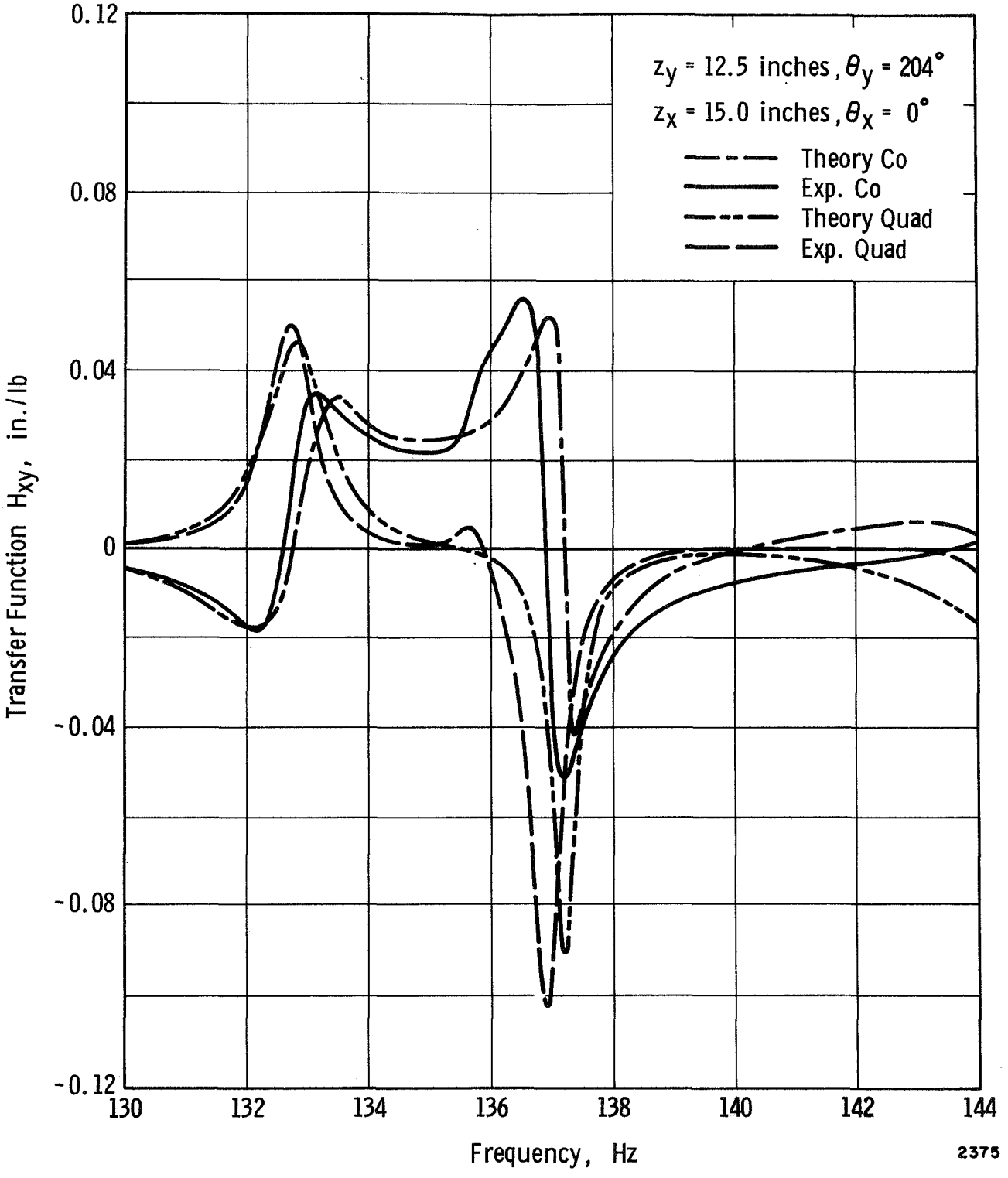

Figure 6. Transfer Function Between Y1 and x = (0,0)

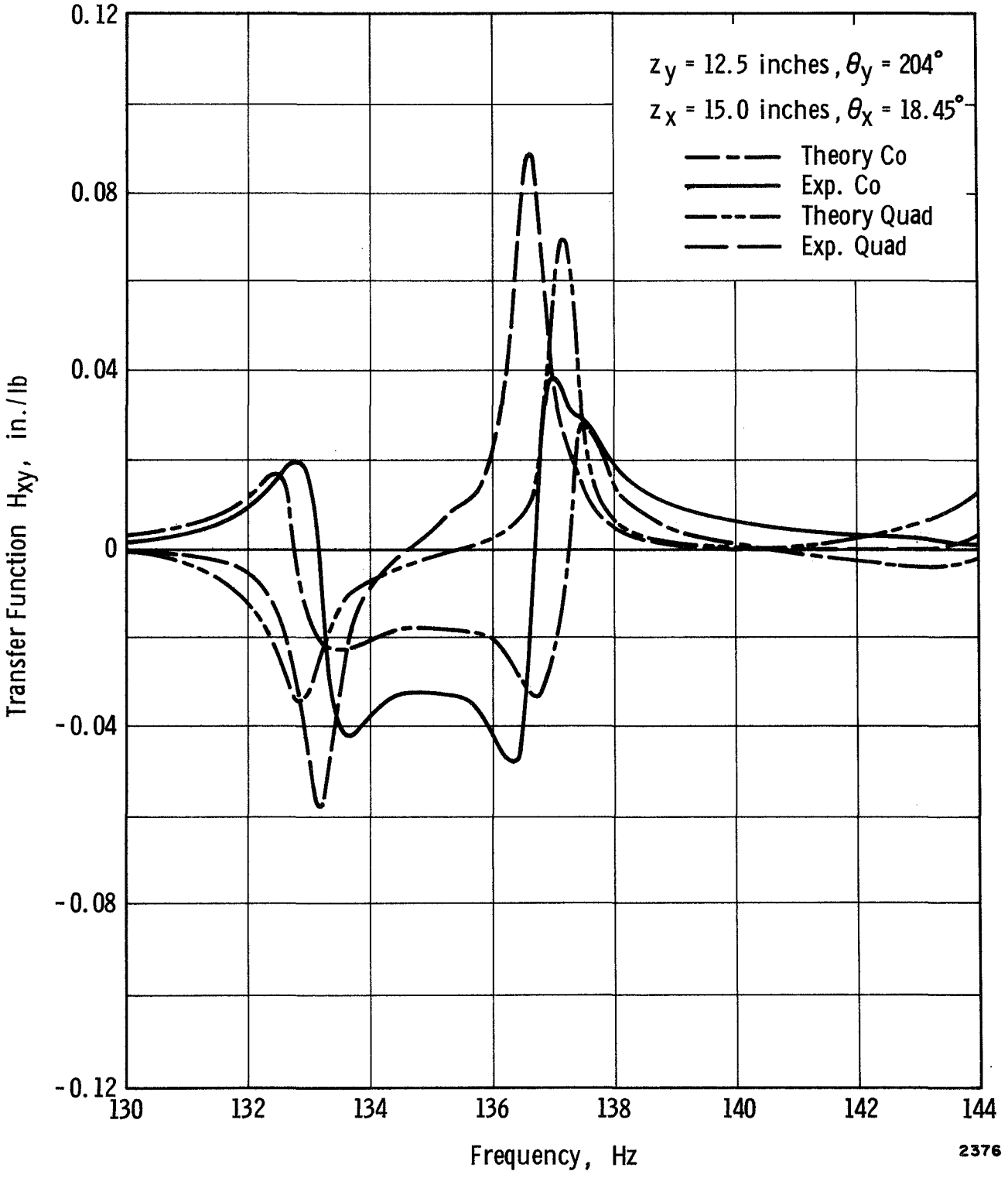

Figure 7. Transfer Function Between Y1 and x = (4,0)

is the same as that for which damping factors are calculated. This type of behavior results from eccentricities in the cylinder.

Distortion in modal response is even more apparent in Figure 8 where a comparison in results is given for the acoustical mobility function between Y1 and harmonic acoustic excitation. Theoretical values are calculated from Eqs. (12), (2), and (10), along with a mesh size of $\Delta = 1/4$ in. Except where stated otherwise, this mesh size was used for all subsequent results. The discrepancy in results evident in Figure 8 indicates that distortion in response patterns are even more prevalent for distributed excitation. Further, evidence of split modes[6] is present, and will be even more apparent in subsequent results.

A similar comparison between theoretical and experimental transfer and acoustic mobility functions is given in Figures 9 - 11 for an additional observation point (Y2). The general behavior is similar to that previously described for (Y1).

Random Excitation and Response

Responses to single-point and acoustic random excitation were determined at the same two observation points which were previously described. The same taped analog random signal whose properties were described in an earlier section were used to drive the cylinder for both types of excitation while response data were simultaneously recorded on analog tape. Subsequent processing of the taped data was accomplished by analog analysis equipment. A speed factor increase of 32 was utilized

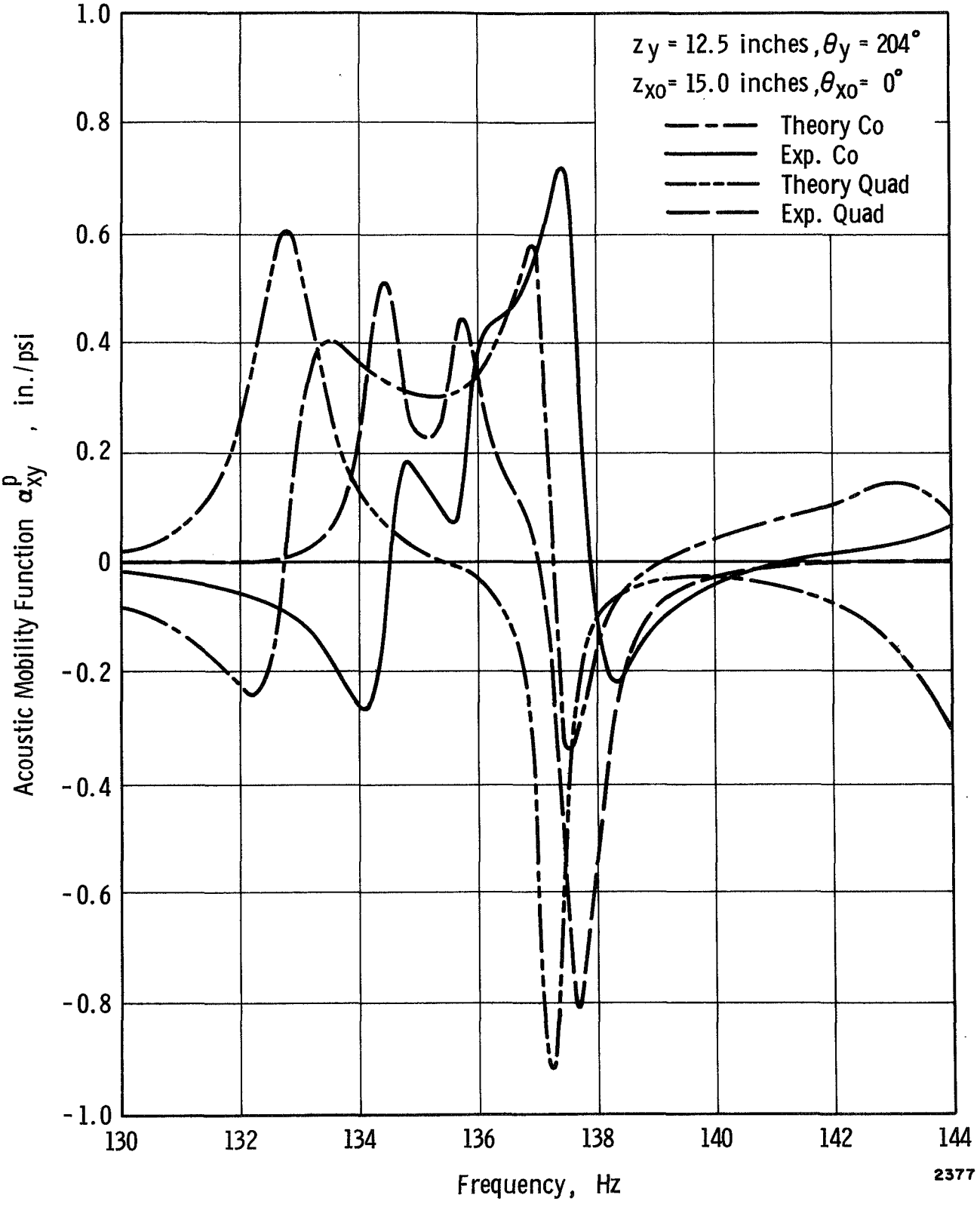

Figure 8. Acoustic Mobility Function For Y1

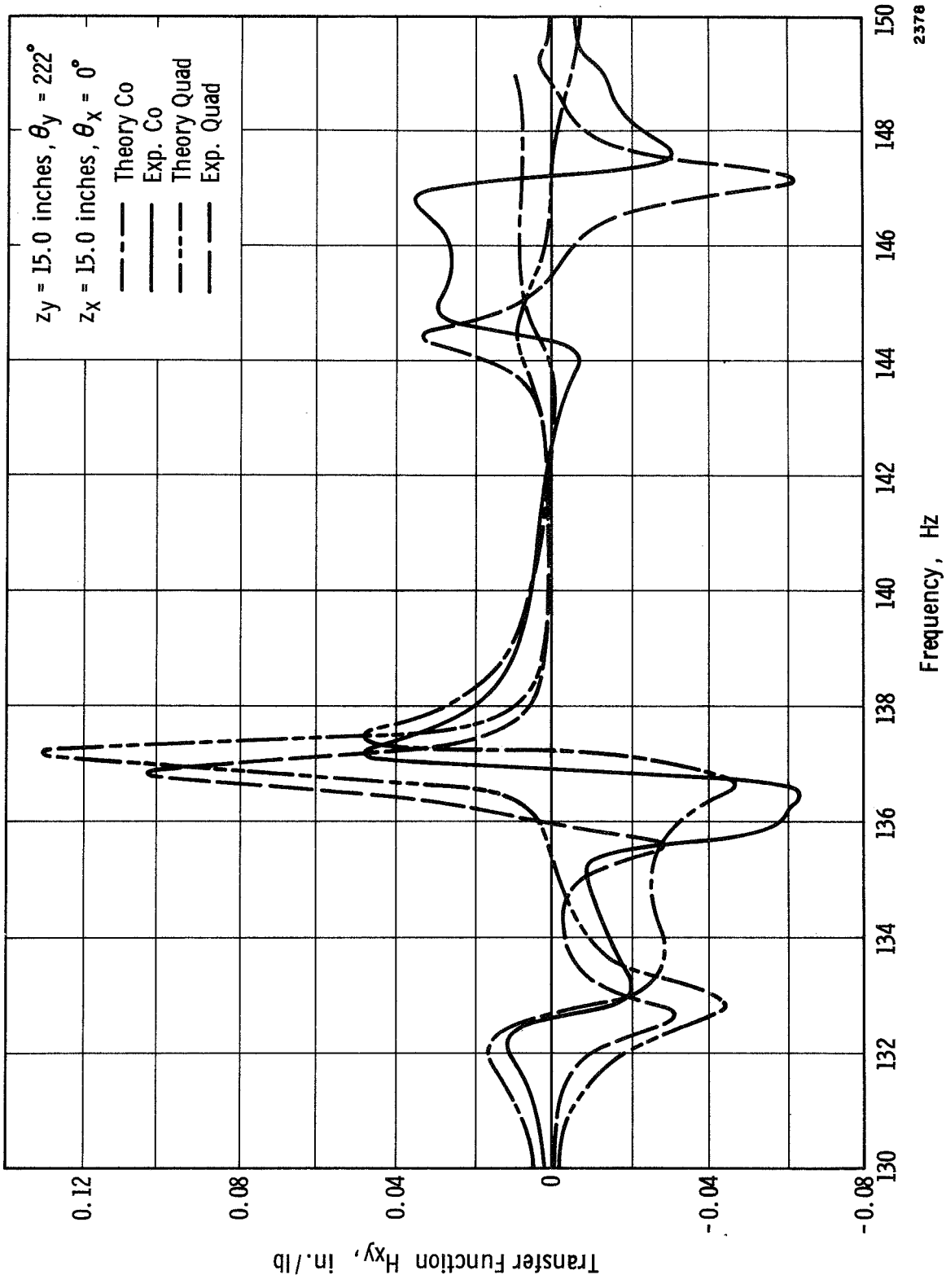

Figure 9. Transfer Function Between Y2 and x = (0,0)

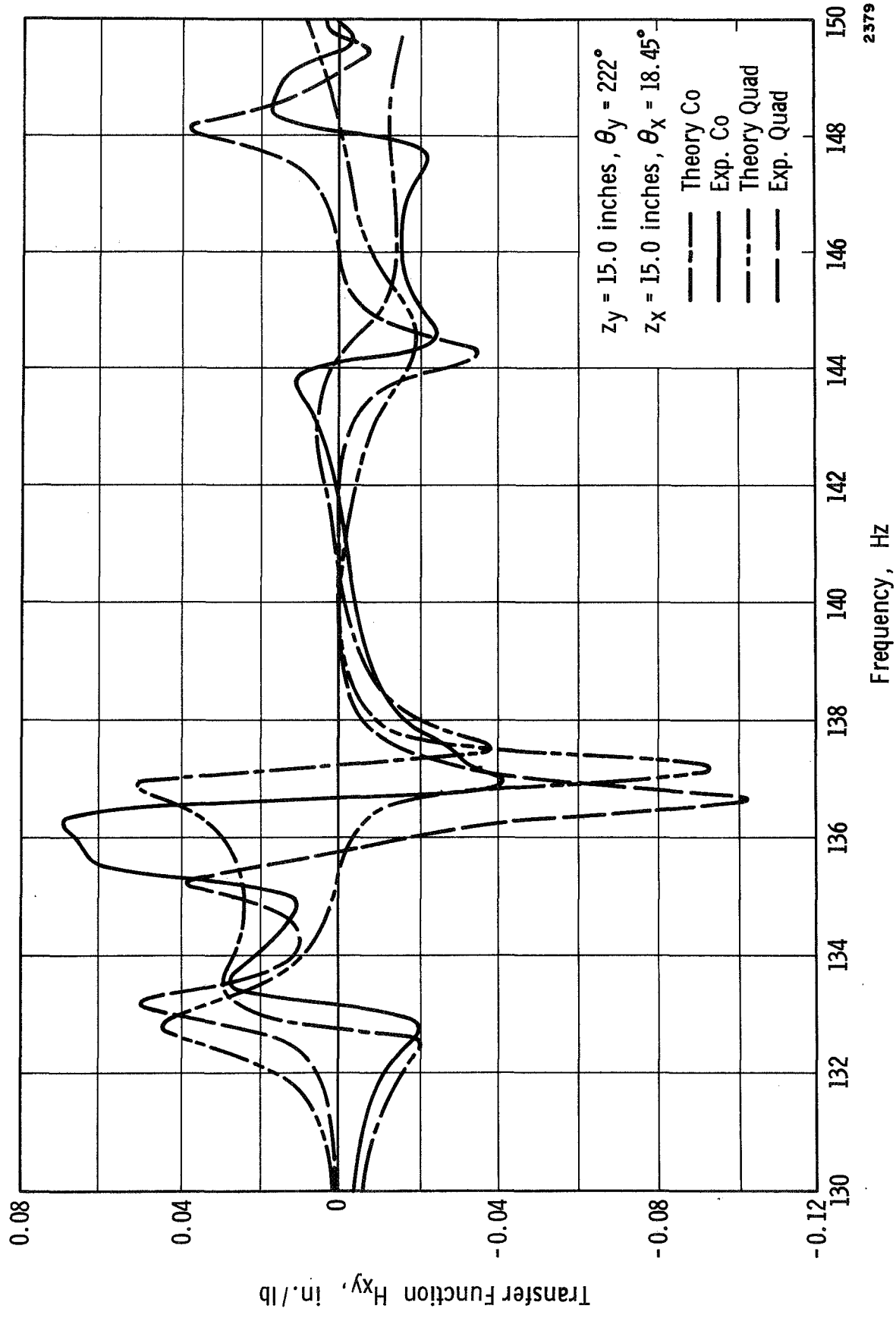

Figure 10. Transfer Function Between Y2 and x = (4, 0)

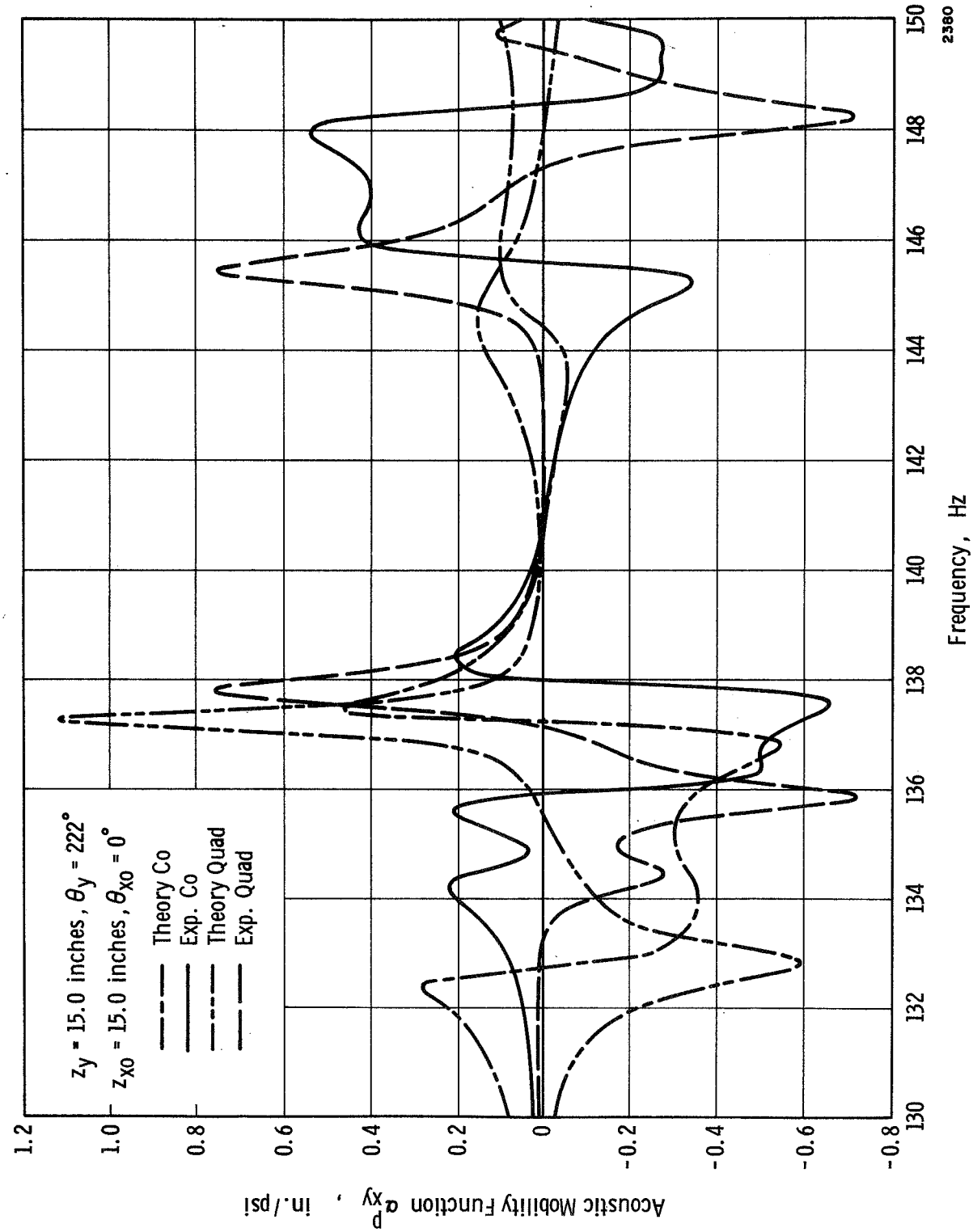

Figure 11. Acoustic Mobility Function For Y 2

in processing response data in order to allow an effective $B_e = 0.312$ Hz with a 10 Hz filter. Results are presented in Figures 12 and 13 respectively. Theoretical results for single-point excitation are based on Eq. (11) in which α_{xy}^{p} is replaced by a single theoretical transfer function H_{xy} between the response and excitation points, and $S_{00}^{p}(f)$ is replaced by $S_{00}(f)$, the input force PSD for this case. Theoretical results for acoustic excitation are based directly on Eq. (11), including the appropriate theoretical expressions which make up α_{xy}^{p} as given by Eq. (12). Average values for $S_{00}^{p}(f)$ and $S_{00}(f)$ were taken as given in a previous section. Semi-experimental values of response are based on a procedure originated by Trubert[7]. That is, the response values are calculated by means of Eq. (11), except that experimentally measured, rather than theoretical, transfer functions or acoustic mobility functions are used as appropriate. For point Y1, these experimental functions have been given in Figures 6 and 8.

It is obvious from Figures 12 and 13 that considerable discrepancy exists between purely theoretical and experimental results. This is not surprising in view of similar discrepancies encountered for the transfer functions. However, it is equally obvious that except for some very slight shift in peak frequencies, quite good comparison is achieved between semi-experimental and experimental results. This indicates that the basic linear random process theory is applicable, so long as good representation of the transfer and acoustic mobility functions can be achieved.

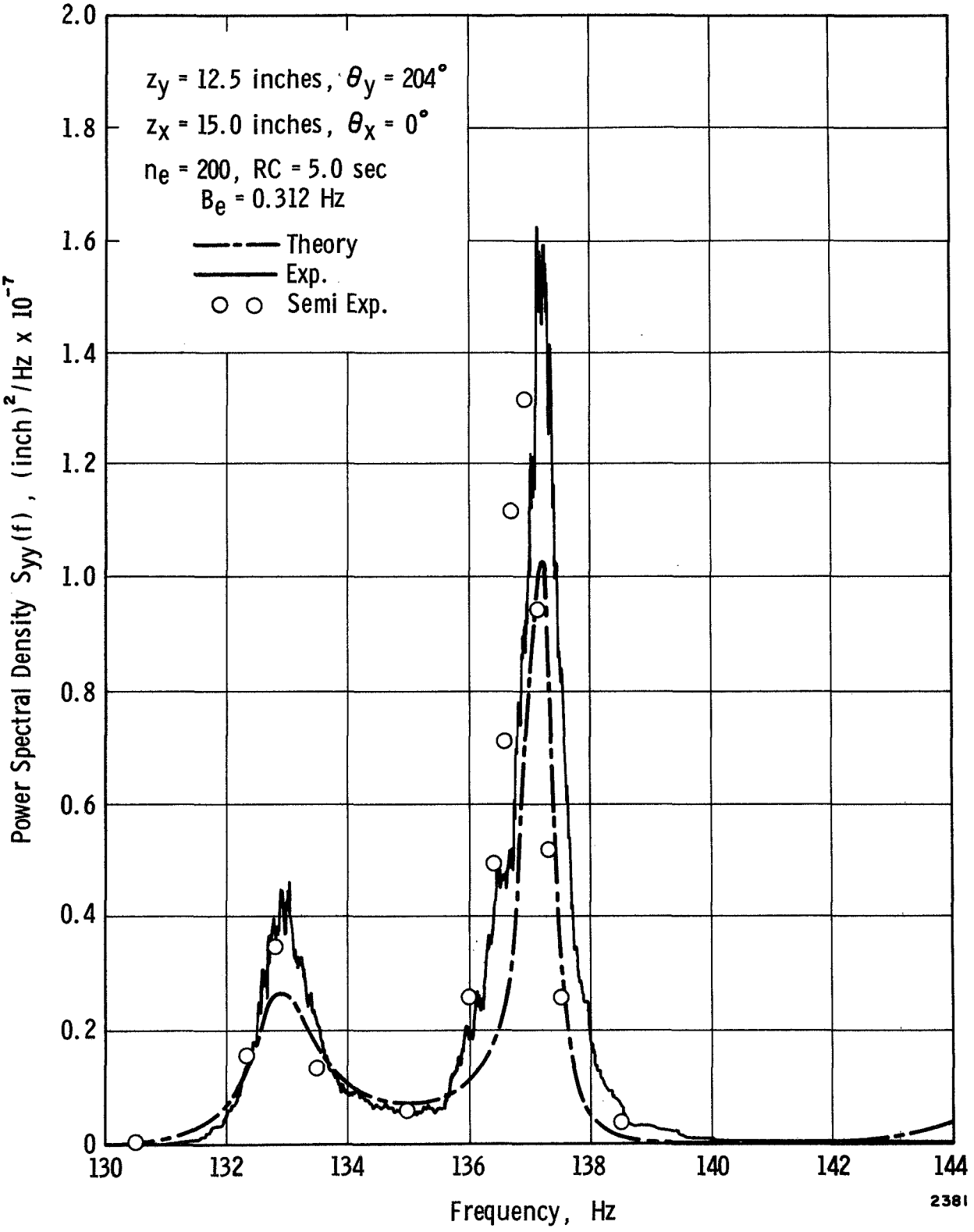

Figure 12. Single Point Random Response For Y1

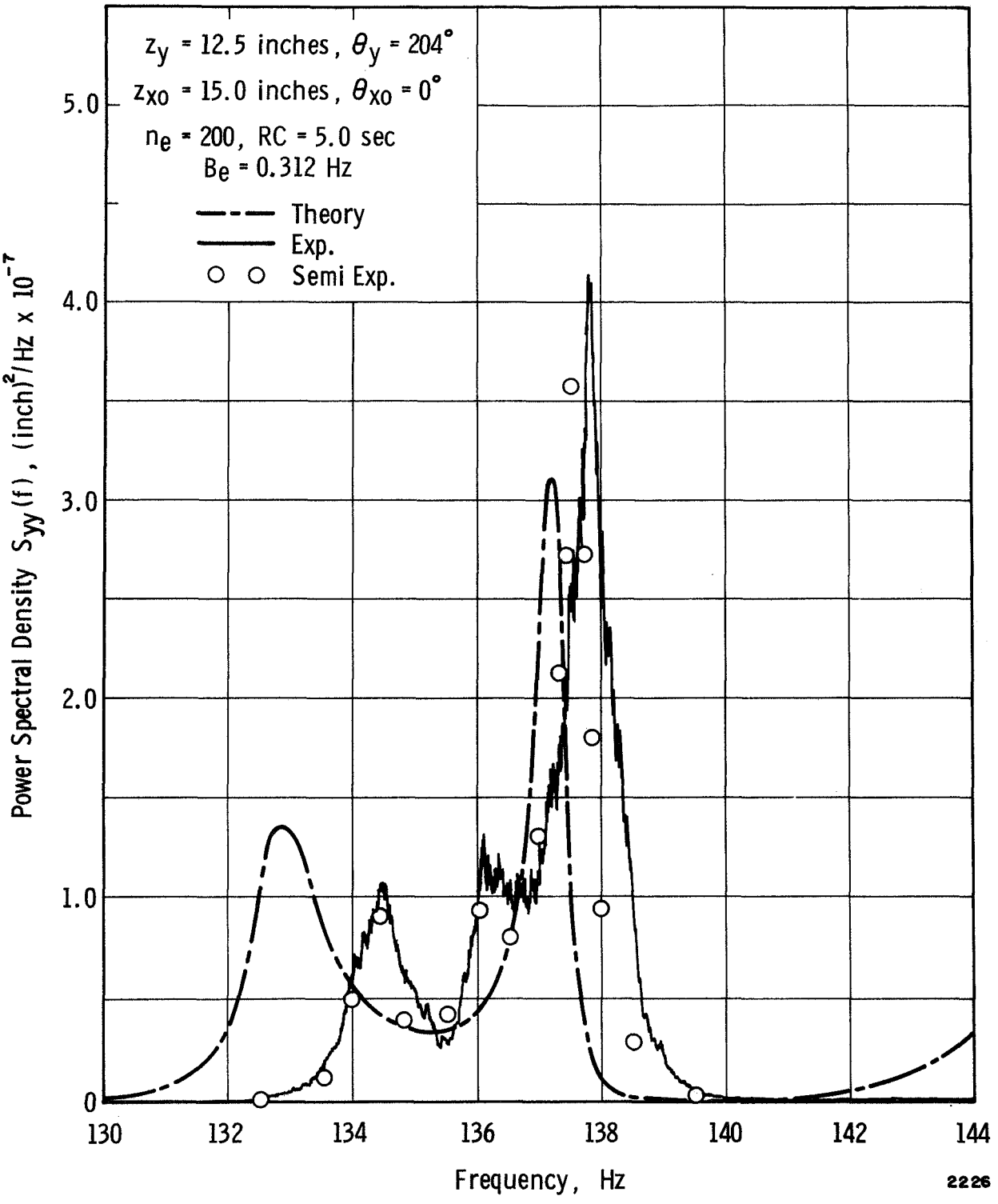

Figure 13. Acoustic Random Response For Y1

In comparing Figures 12 and 13 it can be seen that a partially split mode occurs for the acoustical input between 136 and 138 Hz and similar peak responses occur for slightly different frequencies for the two different kinds of excitation. Such split resonances are even more apparent in Figure 14 where additional response results are given for observation point Y2.

Equivalent force spectra for both points Y1 and Y2 are presented in Figure 15 for purely theoretical data only. The results are based on Eqs. (8a) and (2). More accurate values would be obtained by using purely experimental values in the right side of Eq. (8a). However, the given results are sufficient to indicate the complexity of force spectral density which would be required to simulate the environment. Such complex force spectra are difficult to achieve with present-day electrodynamic shaker equalization equipment.

The influence of mesh size on the theoretical results is indicated in Figure 16 for one typical frequency and observation point Y1. The results are normalized to that for a mesh size of $\Delta = 1/4$ in., which requires 2304 mesh points. The ratio Δ/L is that of mesh size to wave length for the dominant mode of response present, while Δ/r_{max} is mesh size to maximum r_x, which from Figure 4 was taken as 6 inches. It is very interesting that equally valid results can be achieved with a mesh size as coarse as $\Delta = 2$ inches which requires only 144 mesh points. The dependence of this trend on frequency and dominant modal pattern remains to be determined.

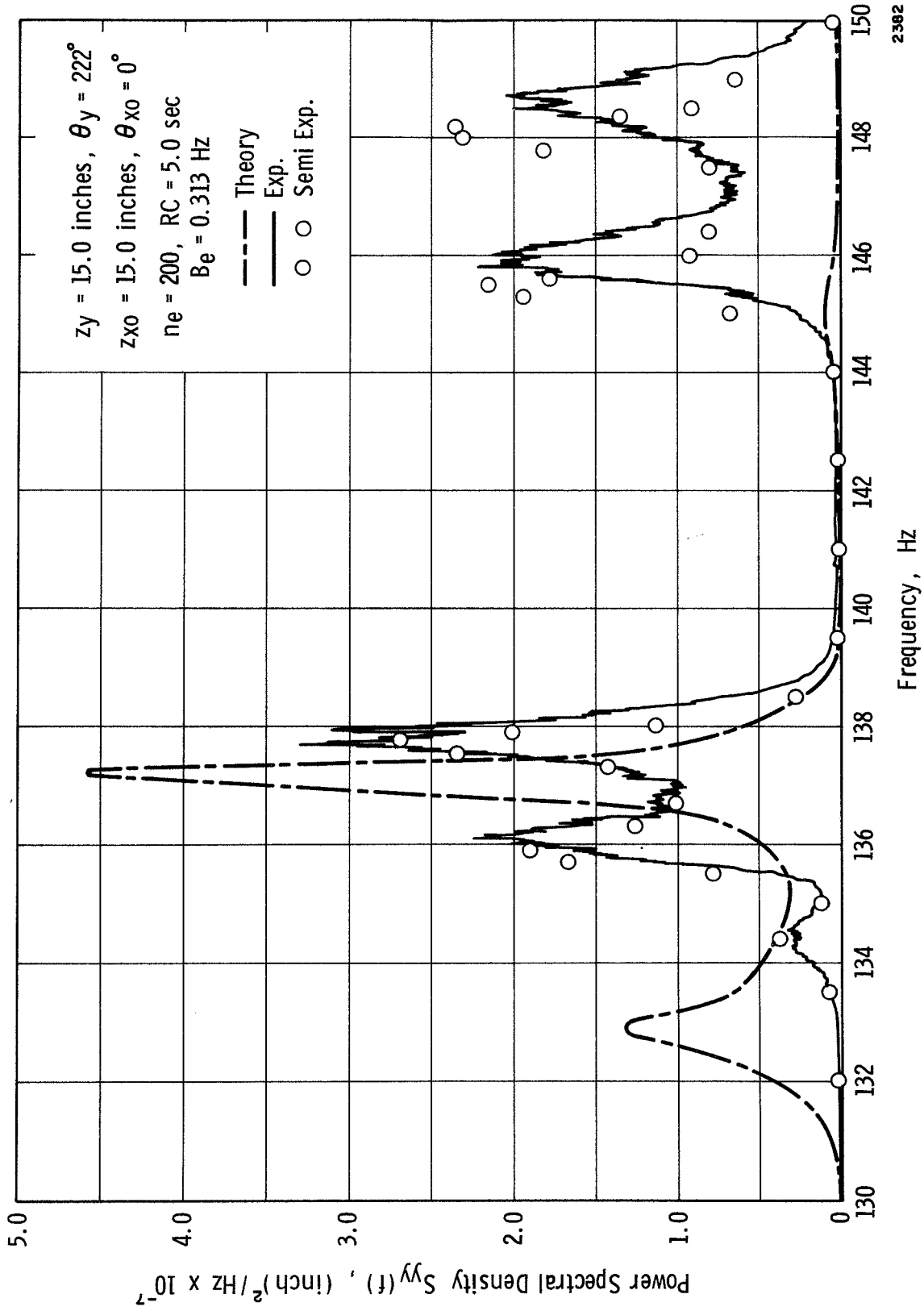

Figure 14. Acoustic Random Response For Y 2

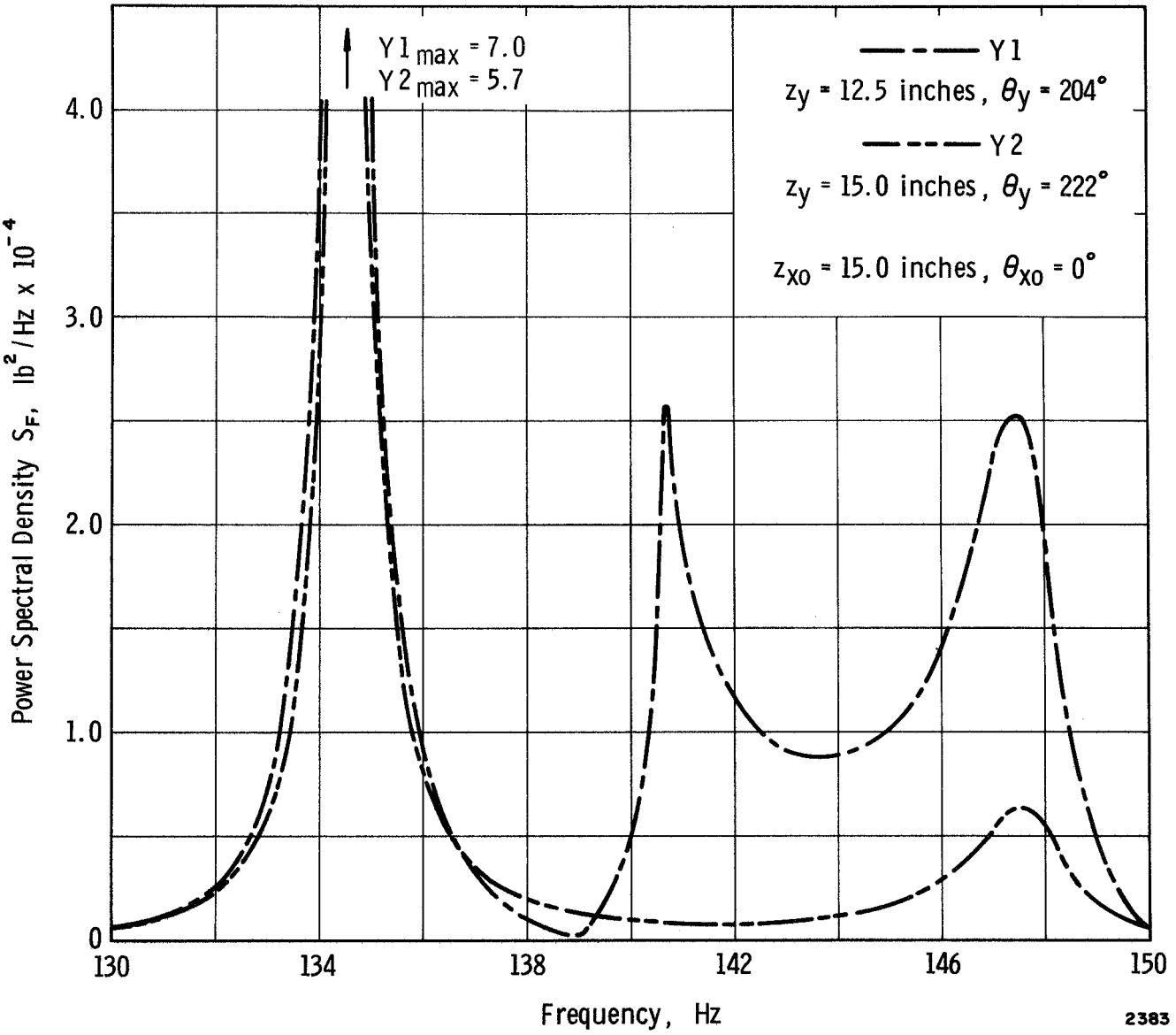

Figure 15. Theoretical Equivalent Force Spectra For Y1 And Y2

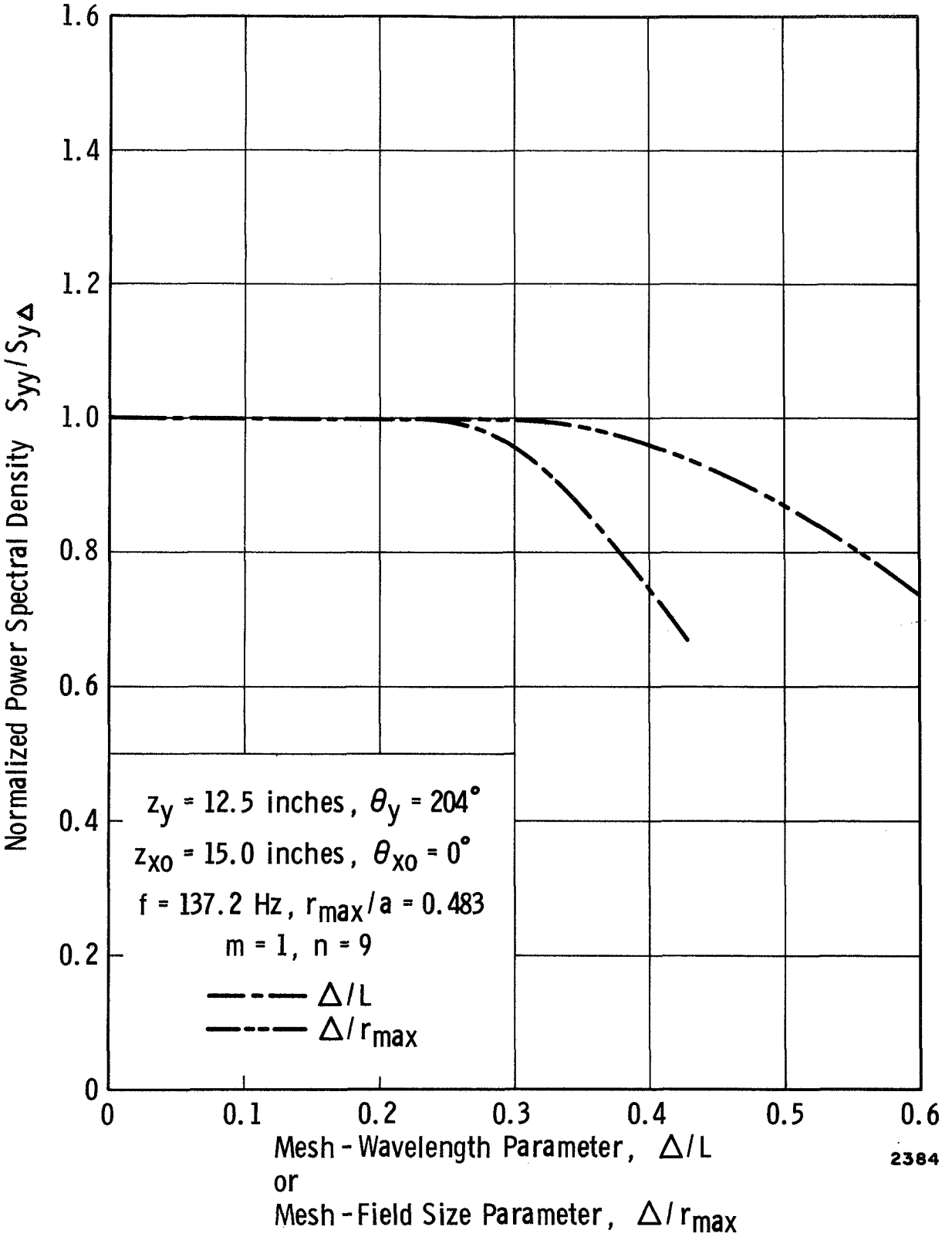

Figure 16. Variation Of Acoustic Response At Y1 With Excitation Mesh Size

A final correlation of purely experimental data is presented in Figure 17, where the ordinary coherence functions[5] have been calculated from

$$\gamma_{xy}^2 = \frac{|S_{0y}(f)|^2}{S_{yy}(f)\ S_{00}(f)}$$

for single point excitation and

$$\gamma_{xy}^2 = \frac{|S_{0y}^p(f)|^2}{S_{yy}(f)\ S_{00}^p(f)}$$

for acoustic excitation. In these expressions $S_{0y}(f)$ and $S_{0y}^p(f)$ is the cross-spectral density measured between the response at y and respectively the force and pressure at $r_x = 0$. These functions should have a value near unity for a perfectly linear system, and will be less than unity otherwise. However, they are highly sensitive to small deviations, and often a value of $\gamma_{xy}^2 \geq 0.6$ is a fair indication of linearity. It should be mentioned that for the acoustical input, an ordinary coherence value near unity is not necessarily an indication of linearity. However, as shown in the Appendix, it does provide such an indication in the present case where the excitation field is of the special convective form. In general, from Figure 17 it can be concluded that excellent linearity is indicated for single point random excitation, while somewhat diminished linearity is suffered for acoustic random excitation. These results appear generally to agree with the data previously presented.

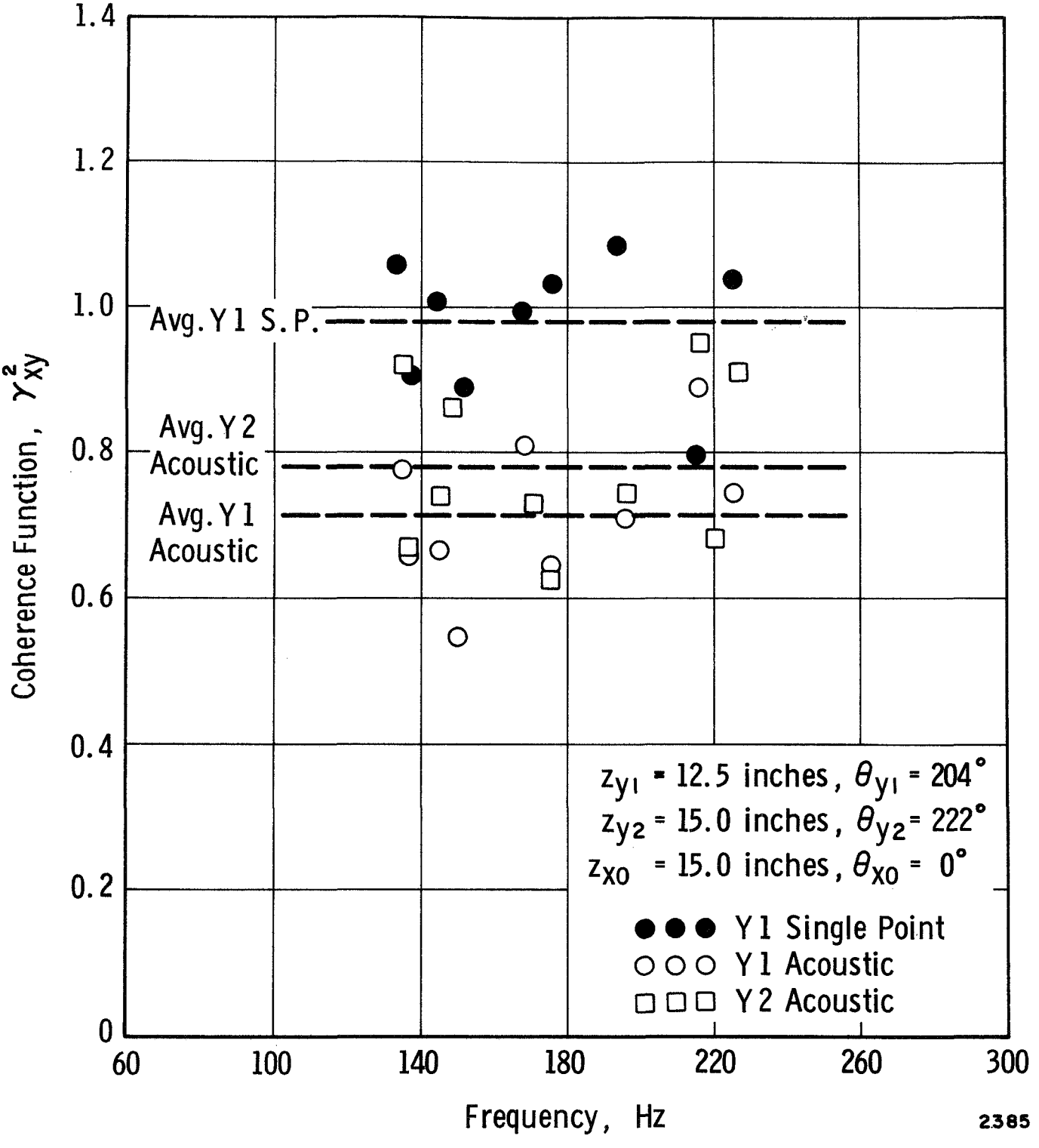

Figure 17. Coherence Function For Random Excitation

ACKNOWLEDGMENTS

The author wishes to express his sincere appreciation to several of his colleagues for help throughout the conduct of this program. Special mention should be given to Mr. Thomas Dunham and Mr. Dennis Scheidt for aiding with the experiments, to Dr. Wen-Hwa Chu for theoretical discussions, and to Mr. Robert Gonzales for digital computer programing.

REFERENCES

1. Robson, J. D., AN INTRODUCTION TO RANDOM VIBRATION, Edinburgh University Press, Edinburgh, Elsevier Publishing Company, New York, 1964.

2. Nemat-Nasser, S., "On the Response of Shallow Thin Shells to Random Excitations," AIAA Journal, 5, 7, pp. 1327-1331, July, 1968.

3. Hwang, Chintsun, "Random Acoustic Response of a Cylindrical Shell," Proceedings of AIAA Structural Dynamics and Aeroelasticity Specialist Conference, New Orleans, La., pp. 112-120, April, 1969.

4. Kana, D. D. and Gormley, J. F., "Longitudinal Vibration of a Model Space Vehicle Propellant Tank," Jour. Spacecraft and Rockets, 4, 12, pp. 1585-1591, Dec., 1967.

5. Bendat, J. S., and Piersol, A. G., MEASUREMENT AND ANALYSIS OF RANDOM DATA, John Wiley & Sons, Inc., New York (1966).

6. Tobias, S. A., "A Theory of Imperfection for the Vibration of Elastic Bodies of Revolution," Engineering, Vol. 172, pp. 409-411, 1951.

7. Trubert, Marc R. P., "Response of Elastic Structures to Statistically Correlated Multiple Random Excitations," Jour. Acous. Soc. Amer., 35, 7, pp. 1009-1022, July 1963.

APPENDIX

Ordinary Coherence Function for Perfectly Correlated Excitation Field

From Reference 5:

$$\{S_{xy}(f)\} = [S_{xx}] \{H_{xy}\}$$

Let point $x = (0, 0)$ be the excitation point for the first element of the column matrices in this expression. Then, in view of Eq. (9b), the first element of the left-hand matrix is

$$S_{0y}(f) = \sum_{i=1}^{N} S_{0i} H_{iy} = \sum_{i=1}^{N} k_{x_i} H_{iy} S_{00}(f)$$

Combining this result along with Eqs. (11) and (12), it is found that

$$\gamma_{0y}^2 = \frac{\left|S_{0y}^p(f)\right|^2}{S_{yy}(f)\, S_{00}^p(f)} = 1$$

The validity of this expression is a joint indication of the linearity of the system as well as an indication of the validity of Eq. (9b) for representing the experimental excitation field.